Published OnlineFirst May 23, 2012; DOI: 10.1158/1535-7163.MCT-12-0037

Preclinical Development

Molecular Cancer Therapeutics

Molecular Mechanisms Involved in the Synergistic Interaction of the EZH2 Inhibitor 3-Deazaneplanocin A with Gemcitabine in Pancreatic Cancer Cells

Amir Avan[1], Francesco Crea[2], Elisa Paolicchi[2], Niccola Funel[3], Elena Galvani[1], Victor E Marquez[4], Richard J. Honeywell[1], Romano Danesi[2], Godefridus J. Peters[1], and Elisa Giovannetti[1]

Abstract

Pancreatic ductal adenocarcinoma (PDAC) is characterized by overexpression of enhancer of Zeste homolog-2 (EZH2), which plays a pivotal role in cancer stem cell (CSC) self-renewal through methylation of histone H3 lysine-27 (H3K27me3). Against this background, EZH2 was identified as an attractive target, and we investigated the interaction of the EZH2 inhibitor DZNeP with gemcitabine. EZH2 expression was detected by quantitative PCR in 15 PDAC cells, including seven primary cell cultures, showing that expression values correlated with their originator tumors (Spearman $R^2 = 0.89$, $P = 0.01$). EZH2 expression in cancer cells was significantly higher than in normal ductal pancreatic cells and fibroblasts. The 3-deazaneplanocin A (DZNeP; 5 μmol/L, 72-hour exposure) modulated EZH2 and H3K27me3 protein expression and synergistically enhanced the antiproliferative activity of gemcitabine, with combination index values of 0.2 (PANC-1), 0.3 (MIA-PaCa-2), and 0.7 (LPC006). The drug combination reduced the percentages of cells in G_2–M phase (e.g., from 27% to 19% in PANC-1, $P < 0.05$) and significantly increased apoptosis compared with gemcitabine alone. Moreover, DZNeP enhanced the mRNA and protein expression of the nucleoside transporters hENT1/hCNT1, possibly because of the significant reduction of deoxynucleotide content (e.g., 25% reduction of deoxycytidine nucleotides in PANC-1), as detected by liquid chromatography/tandem mass spectrometry. DZNeP decreased cell migration, which was additionally reduced by DZNeP/gemcitabine combination (–20% in LPC006, after 8-hour exposure, $P < 0.05$) and associated with increased E-cadherin mRNA and protein expression. Furthermore, DZNeP and DZNeP/gemcitabine combination significantly reduced the volume of PDAC spheroids growing in CSC-selective medium and decreased the proportion of CD133+ cells. All these molecular mechanisms underlying the synergism of DZNeP/gemcitabine combination support further studies on this novel therapeutic approach for treatment of PDACs. *Mol Cancer Ther; 11(8); 1735–46. ©2012 AACR.*

Introduction

With a 5-year survival rate of less than 5%, pancreatic ductal adenocarcinoma (PDAC) is the most lethal among the major solid tumors (1). Despite extensive clinical and scientific efforts, the grim prognosis of this disease has not improved over the past decade (2). The main reasons for the lack of efficient therapeutic strategies include invasive behavior and intrinsic resistance to most chemo/radio- and immunotherapy regimens (3).

Recently, PDAC emerged as a cancer stem cell (CSC)-driven disease. Pancreatic CSCs are highly tumorigenic and have the abilities to self-renew and produce differentiated progeny. Pancreatic CSCs possess the ability to undergo epithelial–mesenchymal transition (EMT; ref. 4) and form spheroids in serum-free medium containing well-defined growth factors. The PDAC spheroids showed increased proliferation, invasiveness, and metastasis (5). CSCs have also been associated with chemoresistance to gemcitabine (6–8). Against this background, studies on key determinants in CSCs can provide both biomarkers of PDAC aggressiveness and optimal novel targets to overcome chemoresistance.

Enhancer of Zeste Homolog-2 (EZH2) is a histone methyltransferase essential for self-renewal of CSCs (9). This protein is the catalytic subunit of Polycomb Repressive Complex 2 (PRC2), 1 of the 2 multimeric repressive complexes in the organization of the Polycomb group (PcG).

Authors' Affiliations: [1]Department of Medical Oncology, VU University Medical Center, Amsterdam, The Netherlands; Departments of [2]Internal Medicine and [3]Surgery, University of Pisa, Pisa, Italy; and [4]Chemical Biology Laboratory, National Cancer Institute, NIH, Frederick, Maryland

Note: Supplementary data for this article are available at Molecular Cancer Therapeutics Online (http://mct.aacrjournals.org/).

A. Avan, F. Crea, and E. Paolicchi equally contributed to this work.

Corresponding Author: Elisa Giovannetti, Department of Medical Oncology, VU University Medical Center, Cancer Center Amsterdam, CCA room 1.52, De Boelelaan 1117, Amsterdam 1081 HV, The Netherlands. Phone: 31-20-4442633; Fax: 31-20-4443844; E-mail: e.giovannetti@vumc.nl and elisa.giovannetti@gmail.com

doi: 10.1158/1535-7163.MCT-12-0037

Published OnlineFirst May 23, 2012; DOI: 10.1158/1535-7163.MCT-12-0037

PcG proteins act as important epigenetic mediators that can repress gene expression by forming multiple complexes leading to histone methylation, resulting in epigenetic control of gene expression (10, 11). In particular, EZH2 can silence several tumor suppressor genes by trimethylation at lysine 27 of histone H3 (H3K27me3; ref. 10), playing an important role in tumor development (12).

EZH2 is overexpressed in many cancer types, including PDACs. Recently, EZH2 expression has been associated with decreased E-cadherin expression and poor prognosis in patients with PDACs (13). Furthermore, Ougolkov and colleagues showed that EZH2 is an important factor in PDAC cell chemoresistance (14). In particular, EZH2 depletion by RNA interference sensitized PDAC cells to gemcitabine (14), which is used in the first-line treatment of PDACs. Because gemcitabine has very limited efficacy (5, 15), novel therapeutic strategies combining gemcitabine with targeted agents against EZH2 are warranted.

Recently, the cyclopentenyl analog of 3-deazaneplanocin A (DZNeP) was identified as a compound capable of reducing the levels of EZH2. This compound is a global histone methylation inhibitor suppressing the activity of *S*-adenosyl-L-homocysteine (AdoHcy) hydrolase, the enzyme responsible for the reversible hydrolysis of AdoHcy to adenosine and homocysteine (16). This results in intracellular accumulation of AdoHcy, which leads to inhibition of the *S*-adenosyl-L-methionine–dependent lysine methyltransferase activity. *S*-adenosyl-methionine metabolism represents a key cellular mechanism for methyl group donation for a variety of methylation-dependent metabolic processes that are disrupted by DZNeP, including production of methyltransferases such as EZH2 (17).

In the present study, we evaluated the EZH2 expression in PDAC tissues and cells and the growth inhibition by DZNeP in combination with gemcitabine in monolayer cell cultures and cells growing as spheroids in serum-free CSC medium. Furthermore, we characterized several factors, including cell-cycle perturbation, apoptosis induction, and inhibition of cell migration, as well as modulation of the expression of several genes involved in the DZNeP/gemcitabine interaction.

Materials and Methods

Drugs and chemicals

DZNeP was provided by Dr. Victor E. Marquez (NCI, NIH, Frederick, MD), whereas gemcitabine was a gift from Eli Lilly Corporation. The drugs were dissolved in sterile water and diluted in culture medium before use. RPMI medium, FBS, penicillin (50 IU/mL), and streptomycin (50 μg/mL) were from Gibco. All other chemicals were purchased from Sigma-Aldrich.

Cell culture

Eight PDAC cell lines (PANC-1, MIA-PaCa-2, BxPc3, Capan-1, PL45, HPAC, HPAF-II, and CFPAC-1), the human pancreatic duct epithelial-like cell line hTERT-HPNE, and skin fibroblasts Hs27 were obtained from the American Type Culture Collection, whereas 7 primary PDAC cultures (LPC006, LPC028, LPC033, LPC067, LPC111, LPC167, and PP437) were isolated from patients at the University Hospital of Pisa (Pisa, Italy), as described previously (18). Cells were cultured in RPMI-1640, supplemented with 10% heat-inactivated FBS and 1% streptomycin/penicillin at 37°C, and harvested with trypsin-EDTA in their exponentially growing phase. The cell lines were tested for their authentication by PCR profiling.

Quantitative real-time PCR

Total RNA was extracted using the TRIREAGENT-LS (Invitrogen), and its yields and purity were checked at 260—to 280 nm with NanoDrop 1000 Detector (NanoDrop Technologies). To prevent RNA degradation, the cells were harvested quickly on ice. One microgram of RNA was reverse-transcribed using the DyNAmo cDNA Synthesis Kit (ThermoScientific), according to the manufacturers' instruction. To evaluate whether the expression of EZH2 was similar in the primary cells and their originator tumors, we also extracted RNA from these 7 tumors, after laser microdissection with a Leica LMD6000 instrument (Leica), using the QIAamp RNA Micro Kit (Qiagen), as described previously (18).

Primers and probes to specifically amplify EZH2, hENT1, CD133, and E-cadherin (Hs01016789_m1, Hs00191940_m1, Hs01009250_m1, and Hs01023894_m1, respectively) were obtained from Applied Biosystems.

The quantitative real-time PCR reactions were carried out in the ABIPRISM 7500 Sequence Detection System instrument (Applied Biosystems).

We conducted a preliminary analysis of 3 housekeeping genes [*β-actin*, glyceraldehyde-3-phosphate dehydrogenase (*GAPDH*), and *β-2-microglobulin*] in all our PDAC cells. Because the values of β-actin were the closest to the geometric mean values of these housekeeping genes, we used this housekeeping gene for the normalization of all the following analyses. Preliminary experiments were carried out to show that the efficiencies of amplification of target and reference genes are approximately equal (18).

Western blotting

To evaluate modulation of EZH2 and H3K27me3 protein expression, the PANC-1, MIA-PaCa-2, and LPC006 cells were treated with 5 μmol/L DZNeP for 72 hours, as reported (19). Blotting procedures were conducted as described previously (18). Membranes were incubated overnight at 4°C with purified mouse anti-EZH2 mAb (BD Biosciences) at 1:1,000 dilution in blocking solution (Rockland in PBS-T), rabbit anti-H3K27me3 (1:1,000; Upstate Biotechnology), rabbit anti-hENT1 and rabbit anti-hCNT1 (1:1,000, kindly provided by M. Pastor-Anglada), and mouse anti-β-actin (1:50,000; Sigma-Aldrich). The membrane was then probed for 1 hour with the goat anti-mouse InfraRed-Dye (1:10,000; Westburg) or goat anti-rabbit InfraRed-Dye (1:10,000; Westburg) secondary antibodies.

Published OnlineFirst May 23, 2012; DOI: 10.1158/1535-7163.MCT-12-0037

Fluorescent proteins were detected by an Odyssey Infrared Imager (LI-COR Biosciences), at 84-μm resolution, 0-mm offset, using high-quality settings. Then, the intensities of protein bands were quantified using the Odyssey v.3.0 Software (LI-COR Biosciences).

Immunocytochemistry

The LPC006 cells were grown in Chamber Slides System (Lab-Tek) in a humidified incubator. After 48 hours, the cells were fixed with 70% ethanol for 10 minutes. Immunocytochemistry was conducted using a monoclonal mouse anti-human E-cadherin antibody (Cell Signaling; EuroClone; 4°C overnight incubation and 1:30 dilution in PBS). Cells were then stained with avidin-biotin-peroxidase complex (UltraMarque HRP Detection). Negative controls were obtained replacing the primary antibody with PBS. The sections were reviewed and scored blindly by comparing the staining of treated cells versus untreated cells (positive control, basal expression), using a system based on staining intensity and on the number of positively stained cells, as described (18).

Growth inhibition studies

Cell growth-inhibitory effects of the DZNeP, gemcitabine, and their combination were studied using the sulforhodamine B assay. Cells were seeded in triplicate at 5×10^3 cells per well and kept at 37°C for 24 hours. Then, the cells were treated for 72 hours with DZNeP (0.001–20 μmol/L), gemcitabine (0.001–500 nmol/L), and DZNeP at fixed concentration of 5 μmol/L simultaneously with gemcitabine (0.001–500 nmol/L). After 72 hours, plates were processed for the sulforhodamine B assay as described earlier (20). To determine whether the drug could kill cells, we also measured optical density on the day of drug addition because cell kill could lead to a decrease in the optical density on day 0. Therefore, for the cell growth inhibition curves, the optical density after 72 hours was corrected for the mean optical density observed for the control wells at the day of drug addition (day 0 value). The 50% growth-inhibitory concentration (IC_{50}) was calculated by nonlinear least-squares curve fitting (GraphPad Prism, Intuitive Software for Science).

Evaluation of synergistic/antagonistic interaction of DZNeP with gemcitabine

The drug interaction of DZNeP and gemcitabine was evaluated by the median drug–effect analysis method originally described by Chou and Talalay (21). Cell growth inhibition of the combination was compared with the cell growth inhibition of each drug alone using the combination index (CI), where CI < 0.9, CI = 0.9–1.1, and CI > 1.1 indicated synergistic, additive, and antagonistic effects, respectively. Data analysis was conducted using CalcuSyn software (Biosoft). Because we considered growth inhibition lower than 50% as not relevant, CI values at fraction affected (FA) of 0.5, 0.75, and 0.9 were averaged for each experiment, and this value was used to calculate the mean between experiments.

Cell-cycle analysis and measurement of cell death

Cell-cycle modulation and cell death induced by treatments with 5 μmol/L DZNeP, gemcitabine at IC_{50} values, and their combination was investigated using 10^5 cells, after 24 and 72 hours, by propidium iodide (PI) staining using a FACSCalibur flow cytometer (Becton Dickinson). Data analysis was conducted with CellQuest (Becton Dickinson), whereas cell-cycle distribution was determined using ModFit (Verity Software), as described (22).

DZNeP, gemcitabine, and their combination were also characterized for their ability to induce cell death by evaluating the sub-G_1 region of the fluorescence-activated cell-sorting analysis (23) and by fluorescence microscopy analysis with bisbenzimide staining (22).

In vitro migration assay (wound-healing assay)

Migration was evaluated using the Leica DMI300B (Leica) migration station integrated with the Scratch Assay 6.1 software (Digital Cell Imaging Labs). Briefly, cells were plated at a density of 3×10^4 cells per well onto 96-well plates, and, after 24 hours, artificial wound tracks were created by scraping with a specific scratcher within the confluent monolayers. After removal of the detached cells by gently washing with PBS, the cells were fed with fresh medium and exposed to 5 μmol/L DZNeP, gemcitabine at IC_{50}, or their combination. The ability of the cells to migrate into the wound area was assessed by comparing the pixels in the images taken at the beginning of the exposure (time 0), with those taken after 4, 6, 8, 24, and 48 hours.

DZNeP/gemcitabine activity in multicellular spheroids

PANC-1, MIA-PaCa-2, and LPC006 spheroids were established by seeding 10,000 cells/mL in Dulbecco's Modified Eagles' Media (DMEM):F12 + GlutaMAX-I (1:1) with insulin-transferrin-selenium (1:1,000; Gibco, Invitrogen), in 24-well ultra-low attachment plates (Corning), according to manufacturers' protocol, as described earlier (24). Spheroids were generated for 10 to 14 days and then harvested for growth inhibition studies in 96-well plates, as well as for RNA isolation.

After checking their growth rate and stability, the spheroids were treated with 5 μmol/L of DZNeP, IC_{50} values of gemcitabine, and their combination for 72 hours. The cytotoxic effects were evaluated by measuring the size and number of spheroids with the microscope Leica DMI300B (Leica), taking 9 pictures for each well. Spheroid volume (V) was calculated from the geometric mean of the perpendicular diameters $D = (D_{max} + D_{min})/2$, ($V = 4/3\pi (D/2)3$).

Liquid chromatography/tandem mass spectrometry measurement of adenosine and phosphorylated deoxynucleosides

Analysis by liquid chromatography/tandem mass spectrometry (LC/MS-MS) was used to determine total cytosolic adenosine as well as total phosphorylated

Published OnlineFirst May 23, 2012; DOI: 10.1158/1535-7163.MCT-12-0037

deoxynucleosides. The latter was calculated from the difference before and after alkaline phosphatase treatment, as described previously (25). Approximately, 2×10^6 cells were seeded into 6-well plates and exposed to either 5 μmol/L DZNeP, gemcitabine at IC_{50} values, or DZNeP/gemcitabine combination for 24 hours, before being snap-frozen as a pellet. Cell pellets were resuspended in a known aliquot of phosphate buffer and precipitated with excess isopropyl alcohol. The supernatant was removed and evaporated to dryness via freeze drying. The dry samples were reconstituted in 200 μL of water, and 20 μL aliquots were used for analysis. The remaining samples were treated quantitatively with alkaline phosphatase (4 units) at 37°C overnight. Chromatography was conducted using a Dionex Ultimate 3000 micro HPLC coupled via a Turbo spray ionization source to a SCIEX API 3000 mass spectrometer (Applied Biosystems). Data analysis was conducted with v.1.52 Analyst software (AB Sciex) controlled by Dionex Mass Spectrometry Link combined with Chromeleon management software modules (ThermoScientific).

Statistical analysis

All experiments were carried out in triplicate and repeated at least twice. Data were expressed as mean values ± SE and analyzed by the Student *t* test or ANOVA followed by the Tukey multiple comparison test. The level of significance was $P < 0.05$.

Results

EZH2 overexpression and modulation by DZNeP

The mRNA expression of EZH2 was detectable in all PDAC cells, as well as in the originator tissues of the primary tumor cell cultures. This expression differed among cells, ranging from 0.100 arbitrary units (a.u.) in LPC006 cells to 0.644 a.u. in PL45 cells (Fig. 1A). The mean expression in the tumor cells (0.372 ± 0.174 a.u.) was similar to the median (0.360 a.u.) and significantly higher ($P < 0.01$) than the expression detected in hTERT-HPNE cells (0.037 a.u.) and in fibroblasts (0.027 a.u.).

EZH2 gene expression in the 7 primary tumor cells and their originator tumors showed a similar pattern and were highly correlated with Spearman analysis ($R^2 = 0.89$, $P = 0.01$).

PANC-1, MIA-PaCa-2, and LPC006 cells were selected for further studies because of previous studies on expression of the CD133 CSC marker (24, 26) and their differential levels of EZH2.

The expression of EZH2 was also studied at protein level, both in untreated cells and in cells treated with 5 μmol/L DZNeP for 24 or 72 hours. As shown in Fig. 1B,

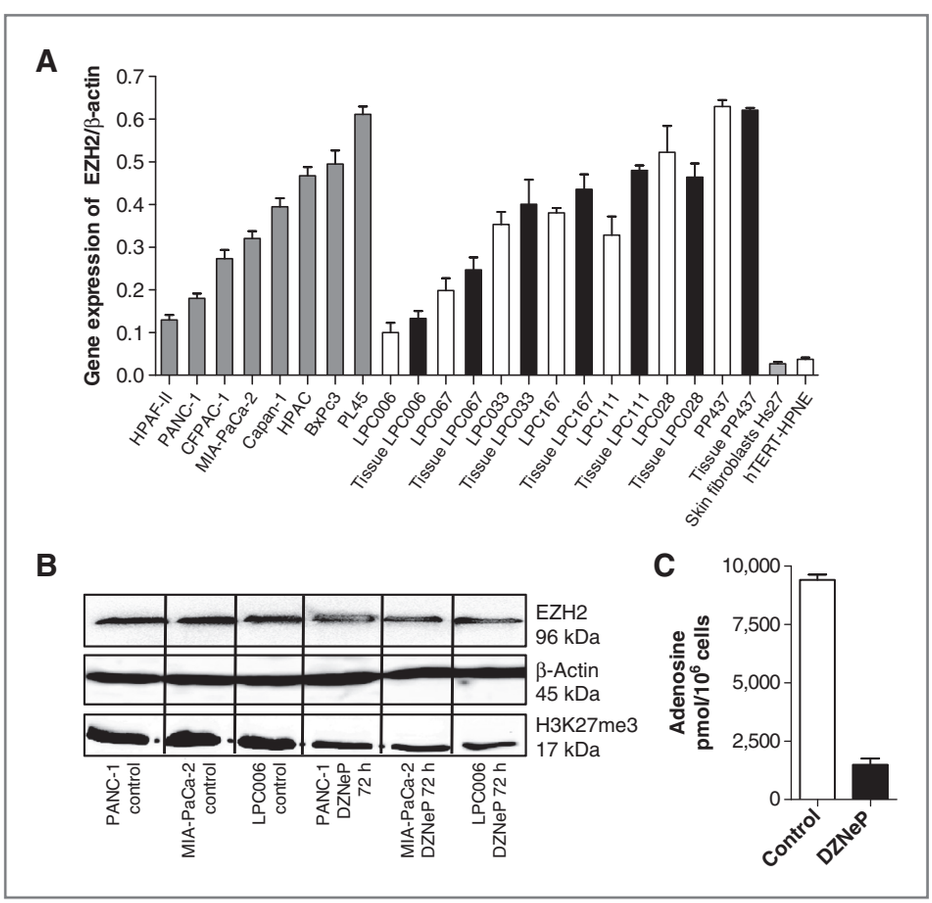

Figure 1. EZH2 expression and DZNeP activity in PDAC cells. A, EZH2 mRNA expression in cell lines (gray bars), primary tumor cultures (white bars), and their originator tissues (black bars). B, effect of 5 μmol/L DZNeP on the expression of EZH2 and H3K27me3 after 72 hours. C, modulation of adenosine by 5 μmol/L DZNeP after 72 hours, as detected by LC/MS-MS. Columns, mean values obtained from 3 independent experiments. Bars, SEM.

Published OnlineFirst May 23, 2012; DOI: 10.1158/1535-7163.MCT-12-0037

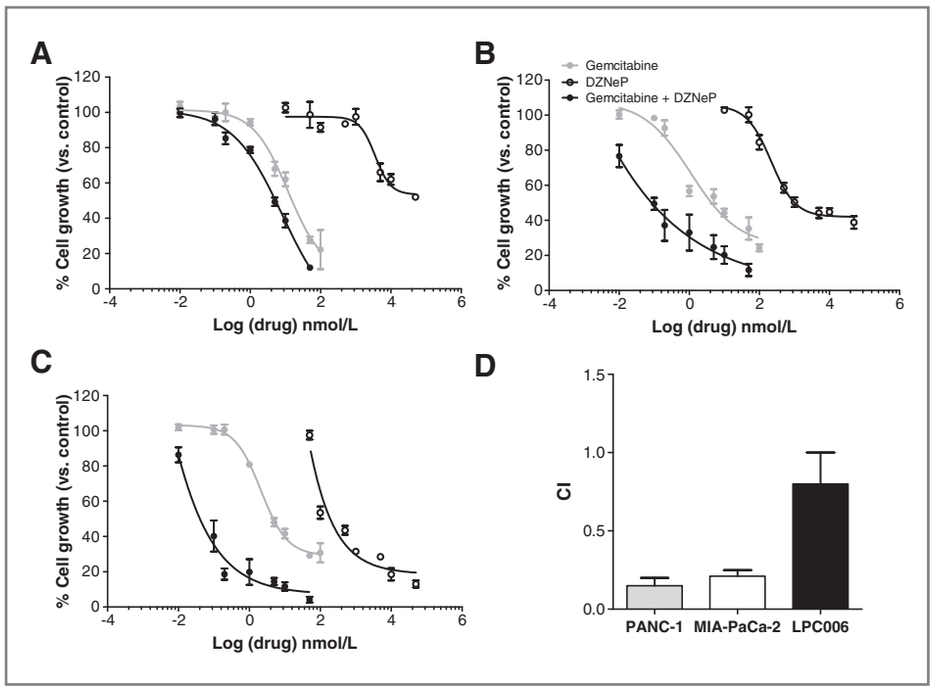

Figure 2. Inhibition of cell proliferation and pharmacologic interaction of DZNeP and gemcitabine. Representative curves of growth-inhibitory effects after 72-hour exposure to 5 μmol/L DZNeP, gemcitabine at IC_{50}, or their combination (drug concentrations on the *x*-axis are referred to gemcitabine) in PANC-1 (A), MIA-PaCa-2 (B), and LPC006 (C). D, mean CI of the DZNeP/gemcitabine combination. CI values at FA of 0.5, 0.75, and 0.9 were averaged for each experiment, and this value was used to calculate the mean between experiments as described in Materials and Methods. Points and columns, mean values obtained from 3 independent experiments; bars, SEM.

DZNeP reduced the expression of EZH2, especially after 72 hours (e.g., 48%, 32%, and 36% reduction of EZH2 in PANC-1, MIA-PaCa-2, and LPC006 cells, respectively). In addition, we investigated the expression of the H3K27me3 protein, which was also reduced after 72-hour exposure.

Finally, as previous studies reported that DZNeP is an *S*-adenosyl-homocysteine hydrolase inhibitor, we verified this inhibition and measured the intracellular concentration of its product adenosine in PANC-1 cells by a specific LC/MS-MS method (16). Adenosine was significantly reduced after 72-hour exposure to DZNeP (Fig. 1C), indicating that *S*-adenosyl-homocysteine hydrolase was significantly inhibited.

Synergistic interaction of DZNeP with gemcitabine

Treatment with DZNeP showed minimal growth inhibition in PANC-1 cells. More than 50% of these cells were still growing after exposure at the highest concentration (20 μmol/L). MIA-PaCa-2 and LPC006 cells were much more sensitive, with IC_{50} values of 1.0 ± 0.3 and 0.10 ± 0.03 μmol/L, respectively (Fig. 2A–C). On the contrary, gemcitabine was highly cytotoxic, with IC_{50} values of 17.9 ± 1.3 nmol/L (PANC-1), 5.9 ± 0.8 nmol/L (MIA-PaCa-2), and 7.2 ± 1.3 nmol/L (LPC006).

On the basis of these results, as well as the modulation of EZH2 protein by 5 μmol/L DZNeP, combination studies were conducted using a fixed concentration of DZNeP at 5 μmol/L. DZNeP enhanced the antiproliferative activity of gemcitabine, reducing the IC_{50} values of gemcitabine to 5.02 ± 1.31, 0.12 ± 0.04, and 0.03 ± 0.01 nmol/L in PANC-1, MIA-PaCa-2, and LPC006. The mean CI showed slight-to-moderate synergism in LPC006 cells, and strong synergism in the PANC-1 and MIA-PaCa-2 cells (Fig. 2D).

To evaluate the mechanisms underlying this synergistic interaction, several biochemical analyses were conducted with the simultaneous combination, as detailed below.

DZNeP/gemcitabine combination enhanced apoptosis

DZNeP, gemcitabine, and their combination affected the cell cycle of PDAC cells (Table 1). In particular, DZNeP significantly reduced the percentage of PANC-1 cells in the G_2–M phase from 27% to 19%, after 72 hours, whereas gemcitabine increased cells in G_2–M phase to 36% ($P < 0.05$). The drug combination significantly reduced the percentage of cells in the G_2–M phase. Hence, DZNeP blocked PANC-1 cells in the G_1–S boundary. Conversely, gemcitabine reduced the cells in this phase, and no modulation was detected after drug combination in the PANC-1 cells. Similar perturbations of the cell cycle were observed in MIA-PaCa-2 cells. However, in LPC006, the percentage of cells in the G_2–M phase was significantly reduced both after DZNeP alone and DZNeP/gemcitabine combination. Moreover, the DZNeP/gemcitabine combination significantly increased cells in the S-phase while reducing cells in the G_0–G_1 phase.

Analysis of the sub-G_1 region showed that drug treatments significantly enhanced cell death compared with control (Table 1). In particular, MIA-PaCa-2 cells treated with the combination exhibited the largest sub-G_1 signal (e.g., 34%).

Further analysis with fluorescence microscopy showed that cells exposed to DZNeP, gemcitabine, and their combination presented a typical apoptotic morphology with cell shrinkage, nuclear condensation and fragmentation, and rupture of cells into debris, after 72-hour

Published OnlineFirst May 23, 2012; DOI: 10.1158/1535-7163.MCT-12-0037

Table 1. Effects of gemcitabine, DZNeP, and their combination on cell-cycle distribution and apoptotic index

Cells	Treatment	G_0–G_1 phase (%)	S-phase (%)	G_2–M phase (%)	Apoptotic index
PANC-1	Control	55.2 ± 1	17.7 ± 1.3	27.2 ± 2.2	3.2 ± 0.4
	Gemcitabine	46.4 ± 2.8	17.8 ± 2.8	35.9 ± 5.6	8.7 ± 1.2[a]
	DZNeP	60.4 ± 0.2	20.8 ± 0.2	18.9 ± 0.1	13.0 ± 0.3[a]
	DZNeP + gemcitabine	54.4 ± 1.4	24.5 ± 2.7	21.2 ± 1.3	29.6 ± 2.8[b]
MIA-PaCa-2	Control	60.5 ± 2.6	15.9 ± 0.9	23.5 ± 1.8	3.9 ± 0.9
	Gemcitabine	44.9 ± 0.9	19.7 ± 2.1	35.3 ± 1.2	9.4 ± 1.3[a]
	DZNeP	73.2 ± 2	14.6 ± 1.4	12.2 ± 0.6	16.5 ± 0.9[a]
	DZNeP + gemcitabine	62.8 ± 0.1	25.3 ± 1.0	11.9 ± 0.9	34.1 ± 0.8[b]
LPC006	Control	65.5 ± 1.3	12.5 ± 1.8	22.1 ± 0.4	2.1 ± 0.6
	Gemcitabine	60.9 ± 7.5	11.8 ± 1.1	27.2 ± 8.5	11.8 ± 0.8[a]
	DZNeP	72.2 ± 1	12.4 ± 0.9	15.4 ± 0.1	17.5 ± 1.2[a]
	DZNeP + gemcitabine	52.5 ± 1.7	30.8 ± 1.1	16.8 ± 0.7	29.2 ± 0.4[b]

NOTE: Cells were exposed to IC_{50} values of gemcitabine, 5 μmol/L DZNeP, and their combination.
The apoptotic index was calculated as the percentage from the ratio between the number of cells displaying apoptotic features and the number of counted cells.
[a]$P < 0.05$ with respect to control cells.
[b]$P < 0.05$ with respect to gemcitabine.

exposure. In all cell lines, 5% to 9% of apoptotic cells were observed after gemcitabine treatment, whereas DZNeP exposure was associated with a higher percentage (6%–15%) of apoptotic cells; drug combination significantly increased the apoptotic index with respect to both control cells and gemcitabine-treated cells.

DZNeP/gemcitabine combination inhibited cell migration and upregulated E-cadherin

To investigate the effects of DZNeP, gemcitabine, and their combination on migratory behavior, a scratch assay was conducted in PANC-1, MIA-PaCa-2, and LPC006 cells. After exposure of PANC-1 cells to gemcitabine at IC_{50}, 5 μmol/L of DZNeP and their combination, a significant reduction of migration was observed after 48 hours (Fig. 3A; Supplementary Fig. S1). In particular, the percentages of cellular migration in PANC-1 were approximately 70%, 60%, 53%, and 38%, in untreated, gemcitabine-, DZNeP-, and their combination-treated cells, respectively.

Inhibition of migration of MIA-PaCa-2 and LPC006 with DZNeP or DZNeP/gemcitabine combination was much more effective than in PANC-1 cells (Fig. 3B and C; Supplementary Fig. S1). DZNeP significantly reduced cells migration with respect to controls after 8 hours, with inhibition of about 20% in the reduction of scratch area in LPC006 cells. In addition, the combination was also significantly more effective than DZNeP alone after 48 hours in both MIA-PaCa-2 and LPC006 cells.

Because previous studies suggested that EZH2 repressed E-cadherin expression (27), we investigated whether DZNeP could affect the levels of this target at both mRNA and protein level. DZNeP and its combination with gemcitabine significantly enhanced E-cadherin mRNA expression (Fig. 3D). Similarly, immunocytochemical analysis in LPc006 cells revealed a significant increase of E-cadherin protein staining after exposure to both DZNeP and DZNeP/gemcitabine combination (Fig. 3E; Supplementary Fig. S2).

DZNeP/gemcitabine combination reduced PDAC spheroids and CD133+ cells

Earlier studies illustrated that results of sensitivity to anticancer drugs, including gemcitabine, in 2-dimensional monolayer cell culture models were different from 3-dimensional (3D) culture models (28). Moreover, the use of serum-free CSC medium should select a population harboring CSCs characteristics, which should be selectively targeted by inhibitors of DZNeP. Thus, to determine whether DZNeP would enhance the efficacy of gemcitabine in 3D systems, we tested these drugs in spheroids of PANC-1, MIA-PaCa-2, and LPC006 cells. After 10 days of culture, we transferred in each well of 96-well plates about 10 spheroids that were approximately 500 μm in diameter (Fig. 4A and B). These growing spheroids were exposed to DZNeP, gemcitabine, and their combination for 72 hours. The growth of these spheroids was only slightly inhibited by gemcitabine (Fig. 4C), whereas DZNeP significantly reduced their volume. However, the DZNeP/gemcitabine combination remarkably increased the disintegration of these spheroids, which were significantly reduced in size compared with the spheroids exposed to gemcitabine-alone in all our 3 PDAC models. Spheroids from each treatment group were collected and used for PCR evaluation of CD133, which was significantly higher than in adherent cells (data not shown). This CSC marker

Published OnlineFirst May 23, 2012; DOI: 10.1158/1535-7163.MCT-12-0037

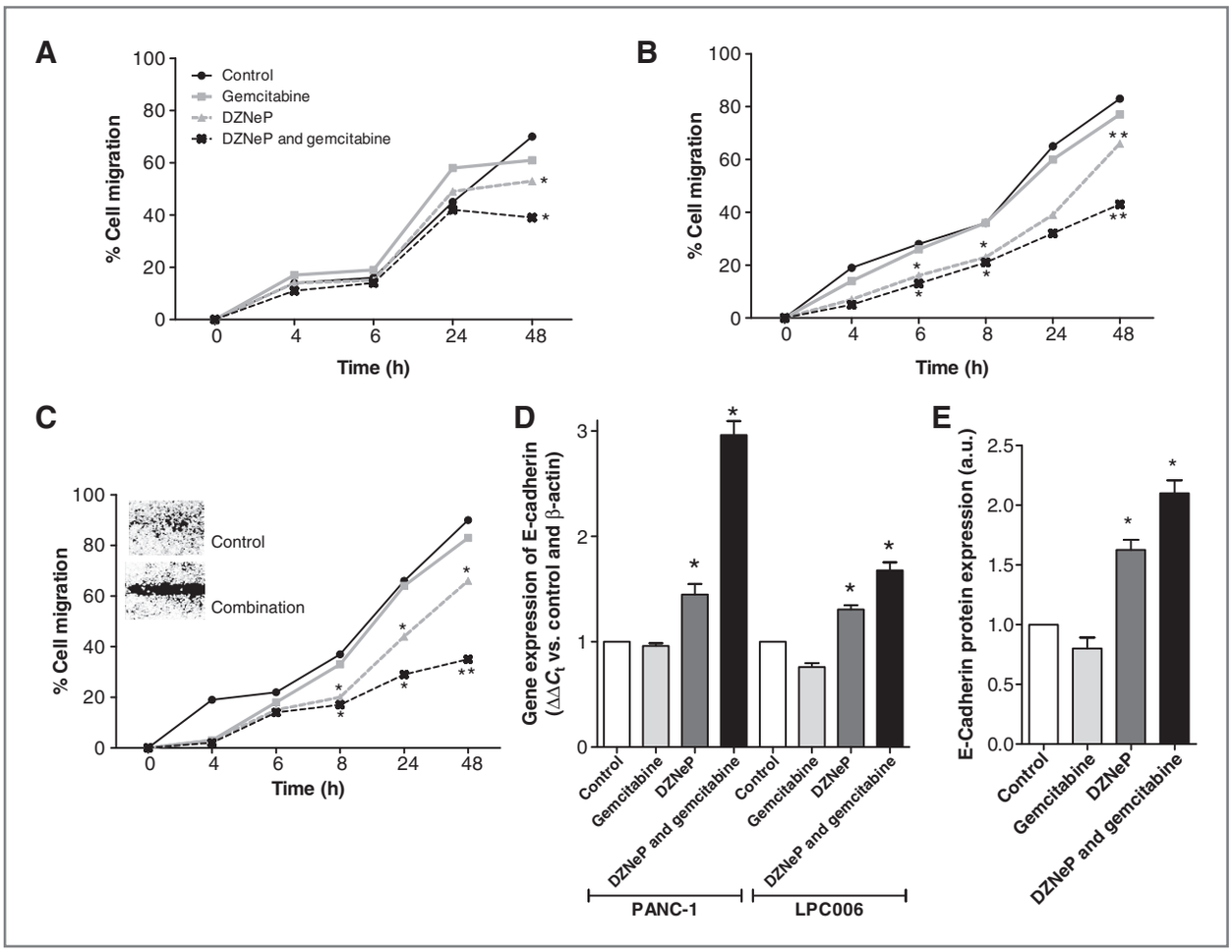

Figure 3. Effects of DZNeP, gemcitabine, and their combination on PDAC cells migration. Results of wound-healing assay in PANC-1 (A), MIA-PaCa-2 (B), and LPC006 (representative picture at 48 hours; C) cells. Cells were exposed to 5 μmol/L DZNeP, gemcitabine at IC_{50}, and their combination. Modulation of E-cadherin after 24 hours as determined by real-time RT-PCR (D) and immunocytochemistry (E). Columns, mean values obtained from 3 independent experiments; bars, SEM. *, significantly different from controls.

was significantly increased after gemcitabine exposure, whereas DZNeP reduced its mRNA levels. Moreover, the DZNeP/gemcitabine combination significantly reduced CD133 expression in both PANC-1 and LPC006 cells, as shown in Fig. 4D.

DZNeP and DZNeP/gemcitabine combination reduced deoxynucleotides and increased hENT1 and hCNT1 expression

Treatment of PANC-1 cells with gemcitabine, DZNeP, and their combination decreased the cellular concentrations of all deoxynucleotides from −25% (dAΣP after DZNeP) to −65% (dAΣP after gemcitabine). Of note, the levels of dTΣP were depleted by all treatments to not detectable levels (Fig. 5A). These changes in the pools of deoxynucleotides were associated with a significant increase in the mRNA expression of hENT1, after exposure to DZNeP and its combination with gemcitabine (Fig. 5B). An increased expression of both hENT1 and hCNT1 transporters was also observed at the protein level (Fig. 5C).

Discussion

The present study shows that the combination of the EZH2 inhibitor DZNeP and the cytotoxic compound gemcitabine was strongly synergistic in a panel of PDAC cells characterized by different molecular properties.

The highly lethal nature of PDAC makes multiple areas of research a priority, including assessment of novel targets that might prevent or suppress the proliferative, invasive, and chemoresistant behavior of PDAC cells.

EZH2 has a master regulatory role in the fate of native embryogenic cells (29), as well as in cancer development via methylation-mediated repression of transcription of several genes (9, 30). Overexpression of EZH2 is a marker of advanced and metastatic disease in many solid tumors,

Published OnlineFirst May 23, 2012; DOI: 10.1158/1535-7163.MCT-12-0037

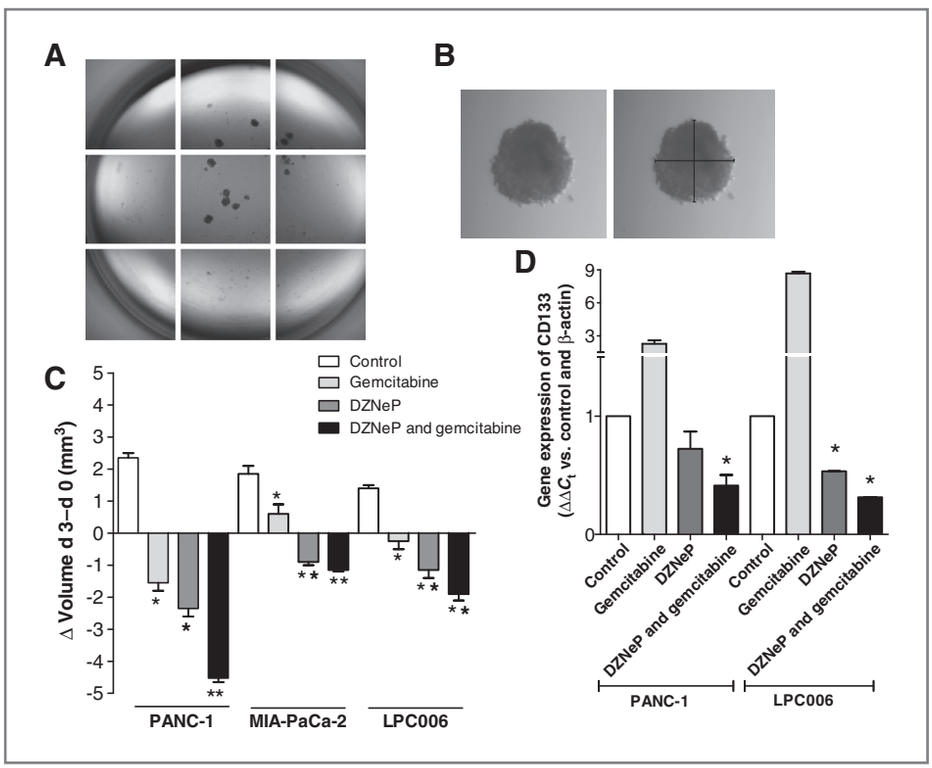

Figure 4. Effects of DZNeP, gemcitabine, and their combinations on PDAC spheroids. Representative pictures of PANC-1 spheroids in a 96-well plate (A), and example (original magnification, ×40) of the measurement of the diameters of one spheroid (B); effect of 5 μM DZNeP, gemcitabine at IC_{50} values, and their combination on the volumes of PDAC spheroids (C) and CD133 mRNA expression (D) after 72-hour exposure. Columns, mean values obtained from 3 independent experiments; bars, SEM. *, significantly different from controls; **, significantly different with respect to gemcitabine.

including PDACs (13, 31, 32), and EZH2 nuclear accumulation is strongly associated with poor differentiation and prognosis of PDACs (13, 14).

Previous studies on PANC-1 and SW1990 showed that suppression of EZH2 expression by RNA interference with lentiviral shEZH2 markedly inhibited cellular proliferation *in vitro* and drastically diminished both tumorigenicity and liver metastasis *in vivo* (33). Furthermore, the transfection of shEZH2 construct cells sensitized MIA-PaCa-2 and Pac04.02 to doxorubicin and

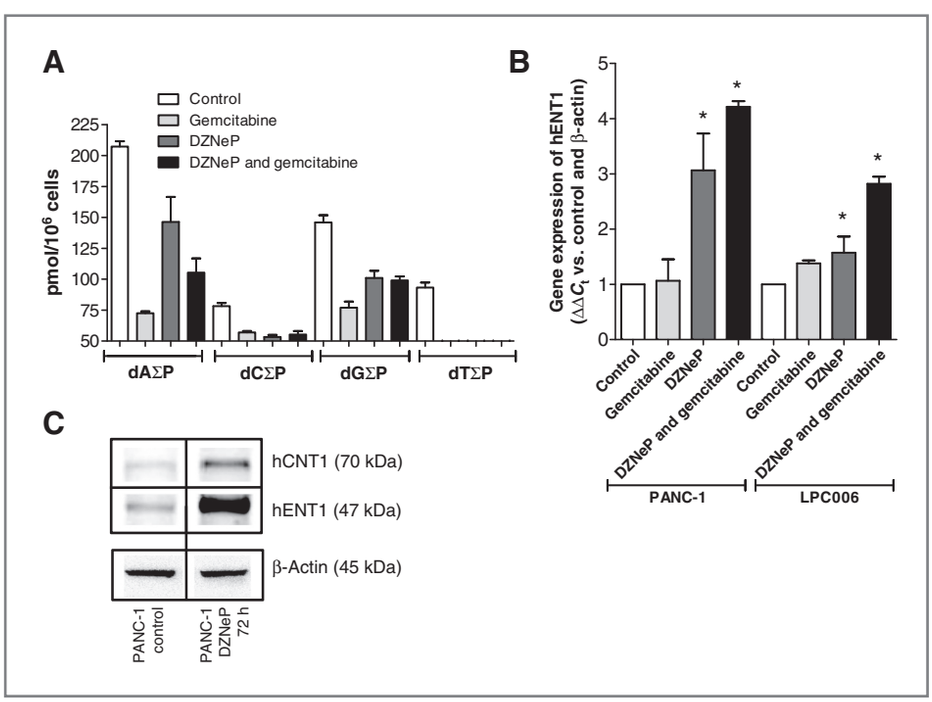

Figure 5. Effects of DZNeP, gemcitabine, and their combination on phosphorylated deoxynucleosides and nucleoside transporters. A, modulation of the intracellular deoxynucleotides, dAΣP (dAMP, dADP, and dATP), dCΣP (dCMP, dCDP, and dCTP), dGΣP (dGMP, dGDP, and dGTP), and dTΣP (dTMP, dTDP, and dTTP), as detected by the LC/MS-MS. Modulation of hENT1 mRNA expression (B) and representative blot of the modulation of hENT1 and hCNT1 protein levels after 72-hour exposure to 5 μmol/L DZNeP (C). Columns, mean values obtained from 3 independent experiments; bars, SEM. *, significantly different from controls.

Published OnlineFirst May 23, 2012; DOI: 10.1158/1535-7163.MCT-12-0037

gemcitabine (14), suggesting that combination of EZH2 inhibitors with gemcitabine might overcome the intrinsic chemoresistance of PDACs.

To our knowledge, this is the first study evaluating the pharmacologic interaction of the small-molecule EZH2 inhibitor DZNeP with gemcitabine in PDAC cells (Fig. 6).

The expression of EZH2 was detectable in all our PDAC cells, including 7 primary tumor cell cultures, in their first passages, where the levels of EZH2 mRNA were comparable with their originator tumors, suggesting that these cells represent optimal preclinical models for our pharmacologic studies. Conversely, EZH2 levels were significantly lower in both fibroblasts and in the normal pancreatic ductal cells HPNE, in agreement with earlier data on normal pancreatic tissue and specimens from patients affected by pancreatitis (13).

Because DZNeP inhibits *S*-adenosyl-homocysteine hydrolase, a component of the methionine cycle, resulting in accumulation of the inhibitory *S*-adenosyl-homocysteine, its effects on histone methylation are global rather than EZH2-specific (31, 34), and we evaluated both the modulation of H3K27me3 expression and the perturbation of intracellular adenosine.

In our PDAC cells, using concentration and exposure time (5 μmol/L, 72 hours) similar to those used in other tumor cells (35), we observed a significant reduction of both EZH2 and H3K27me3 expression, as well as a dramatic decrease of intracellular adenosine content. Although DZNeP alone did not significantly affect proliferation of PANC-1 and MIA-PaCa-2 cells, these data suggested that DZNeP effectively reached its targets.

A recent phase III trial showed that the oxaliplatin/irinotecan/fluorouracil/leucovorin (FOLFIRINOX) regimen is an option for the treatment of metastatic patients with good performance status but was associated with increased toxicity (36). Thus, gemcitabine is still the standard first-line agent (37), and several studies are evaluating novel strategies to improve its activity against PDACs.

In the present study, we showed that DZNeP/gemcitabine combination was synergistic in 2 representative PDAC cell lines, PANC-1 and MIA-PaCa-2, and in the primary cell culture LPC006.

This synergistic interaction against cell proliferation was associated with a significant increase in apoptosis induction. This effect may be related to cell-cycle

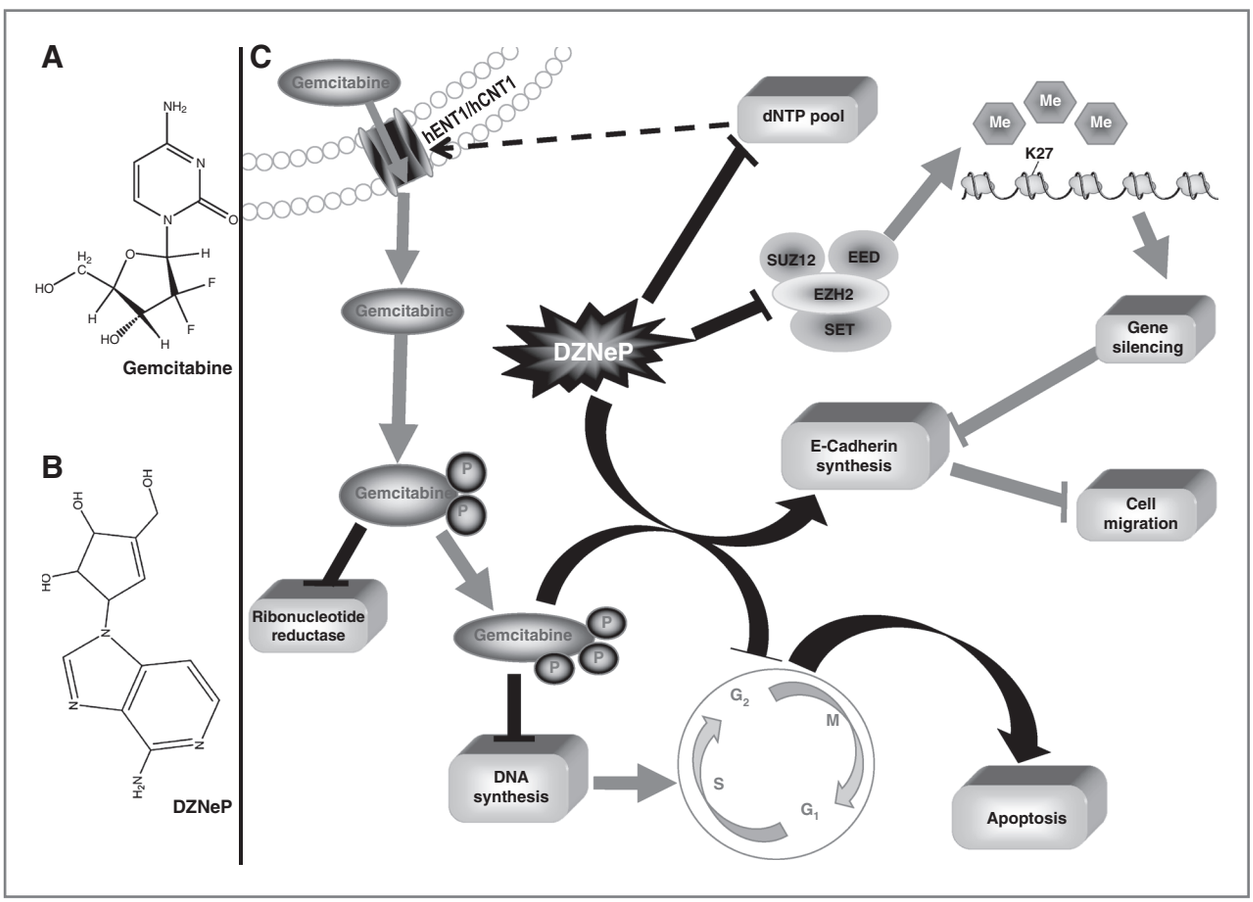

Figure 6. Molecular mechanisms involved in the synergistic interaction of DZNeP with gemcitabine. Structures of gemcitabine (A) and DZNeP (B). C, DZNeP enhanced the growth-inhibitory effects of gemcitabine through its pronounced proapoptotic, anti-invasive effects, as well as by inhibiting spheroid growth. Furthermore, modulation of phosphorylated deoxynucleosides and nucleoside transporters promotes gemcitabine uptake.

Published OnlineFirst May 23, 2012; DOI: 10.1158/1535-7163.MCT-12-0037

modulation, which was also important for the efficacy of the combination of the histone deacetylase inhibitor trichostatin A with gemcitabine (38). Cellular damage induced by chemotherapeutic drugs such as gemcitabine can convert some targets of EZH2 into critical survival factors. In this context, the blockade of EZH2 after the exposure to cytotoxic drugs could prevent cell damage repair, leading to apoptosis. In particular, previous studies in breast cancer cells resistant or sensitive to DZNeP led to the identification of a set of PRC2 target genes including *TGFBI*, *IGFBP3*, and *PPPIR15A*, which are involved in apoptosis (16), whereas TGFB signaling pathway is frequently deregulated in PDACs (39).

However, our findings show that the synergistic interaction of DZNeP with gemcitabine is also mediated by other mechanisms, which reduced PDAC aggressiveness and enhanced sensitivity to gemcitabine.

Because one of the major hallmarks and problems in the therapy of PDACs is its early local and systemic dissemination, we evaluated whether DZNeP might affect cell migration. In agreement with previous studies, showing that inhibition of EZH2 by DZNeP attenuated glioblastoma and mesothelioma cell migration/invasion (36, 40), we observed that inhibition of EZH2 by DZNeP and its combination with gemcitabine significantly reduced cell migration, as detected with wound-healing assay.

Several classes of proteins are participating to invasive PDAC phenotype, including cell–cell adhesion molecules like members of immunoglobulin and calcium-dependent cadherin families and integrins. One widely observed alteration in cell-to-environment interaction in PDAC involves E-cadherin, which couples adjacent cells by E-cadherin bridges, and a recent study showed that recruitment of histone deacetylases 1/2 by the transcriptional repressor ZEB1 downregulates E-cadherin expression in PDACs (41).

Keeping with previous evidence on inverse relationship between EZH2 and E-cadherin expression (13), our data also show that DZNeP-induced EZH2 inhibition resulted in an increase in both mRNA and protein expression of E-cadherin.

Recently, PDACs also emerged as a CSC-driven disease (42). This might at least partially explain its chemoresistant nature (8) and compounds targeting critical developmental genes keeping self-renewal in CSCs, including Sonic hedgehog, BMI-1, and EZH2, seem promising anticancer agents. For example the curcumin analog difluorinated-curcumin inhibited formation of pancreatospheres as well as PDAC growth by switching on several suppressor microRNAs and attenuating EZH2 expression (43).

DZNeP significantly reduced the volume of PDAC spheroids growing in serum-free stem cell medium. Gemcitabine only slightly reduced the volume of these spheroids, possibly by affecting some remaining bulk tumor cells, but it increased the expression of the CSC marker CD133, as observed previously (44), suggesting that exposure to gemcitabine might select a population of more aggressive cells. Conversely, DZNeP was able to effectively deplete the most aggressive subpopulation of PDAC cells, as suggested by the significant reduction of both spheroids and CD133 expression.

In addition to the effects of DZNeP on migration and spheroids, the present study also showed that it interfered with pivotal determinants for the activity of gemcitabine. In particular, different thymidylate synthase inhibitors upregulated hENT1 and increased gemcitabine sensitivity by depleting intracellular nucleotide pools (45, 46). Therefore, we analyzed the cellular deoxynucleotide pools and modulation of the expression of key nucleoside transporters (47). Gemcitabine, DZNeP, and their combination significantly depleted all the endogenous deoxynucleotides. The results achieved after exposure to gemcitabine might be explained by gemcitabine-induced inhibition of ribonucleotide reductase, as reported previously (48). DZNeP is not phosphorylated and does not get incorporated into DNA (49), but it markedly reduced endogenous deoxynucleotides. This might, at least in part, explain the significant upregulation of both hENT1 and hCNT1, potentially facilitating gemcitabine cytotoxicity.

In conclusion, inhibitors of EZH2, such as DZNeP, seem very promising anticancer agents by attacking key mechanisms involved in the proliferation, cell-cycle control, apoptosis, and migration of PDAC cells. Moreover, the favorable modulation of hENT1/hCNT1 transporter makes DZNeP an optimal candidate for combination with gemcitabine. The synergistic results observed in the present study may have critical implications for the rational development of innovative regimens including DZNeP and gemcitabine to improve the efficiency of the actual treatment of PDACs.

Disclosure of Potential Conflicts of Interest

No potential conflicts of interest were disclosed.

Authors' Contributions

Conception and design: A. Avan, F. Crea, E. Paolicchi, G.J. Peters, E. Giovannetti
Development of methodology: A. Avan, E. Paolicchi, N. Funel, E. Galvani, R.J. Honeywell, G.J. Peters, E. Giovannetti
Acquisition of data (provided animals, acquired and managed patients, provided facilities, etc.): A. Avan, N. Funel, E. Galvani, G.J. Peters, E. Giovannetti
Analysis and interpretation of data (e.g., statistical analysis, biostatistics, computational analysis): A. Avan, F. Crea, E. Paolicchi, N. Funel, R.J. Honeywell, E. Giovannetti
Writing, review, and/or revision of the manuscript: A. Avan, F. Crea, E. Paolicchi, E. Galvani, V.E. Marquez, R. Danesi, G.J. Peters, E. Giovannetti
Administrative, technical, or material support (i.e., reporting or organizing data, constructing databases): F. Crea, E. Paolicchi, E. Giovannetti
Study supervision: F. Crea, G.J. Peters, E. Giovannetti
Provided the synthetic material (DZNep): V.E. Marquez

Acknowledgments

The authors thank M. Smits and Dr. T. Wurdinger (Department of Neuro-Oncology, VU University Medical Center, Amsterdam, Netherlands) for their advice on EZH2; Dr. C. Fedrigo (Department of Radiobiology, VU University Medical Center) for his help on experiments with spheroids; and A. Griffioen (Angiogenesis-group, VU University Medical Center) for the migration station to conduct wound-healing assays.

Published OnlineFirst May 23, 2012; DOI: 10.1158/1535-7163.MCT-12-0037

Grant Support

This work was supported by grants from the Netherlands-Organization for Scientific Research (Veni grant #91611046 to E. Giovannetti), AIRC-Marie Curie (International Fellowship to E. Giovannetti), Iran's National-Elites-Foundation (A. Avan), and CCA-VICI foundation (grant #2012-5-07 to A. Avan, G.J. Peters, and E. Giovannetti); and by the Intramural Research Program of the NIH, NCI, Center for Cancer Research (to V.E. Marquez).

The costs of publication of this article were defrayed in part by the payment of page charges. This article must therefore be hereby marked *advertisement* in accordance with 18 U.S.C. Section 1734 solely to indicate this fact.

Received January 16, 2012; revised April 16, 2012; accepted April 27, 2012; published OnlineFirst May 23, 2012.

References

1. Jemal A, Bray F, Center MM, Ferlay J, Ward E, Forman D. Global cancer statistics. CA Cancer J Clin 2011;61:69–90.
2. Ottenhof NA, de Wilde RF, Maitra A, Hruban RH, Offerhaus GJ. Molecular characteristics of pancreatic ductal adenocarcinoma. Patholog Res Int 2011;2011:620601.
3. Hamacher R, Schmid RM, Saur D, Schneider G. Apoptotic pathways in pancreatic ductal adenocarcinoma. Mol Cancer 2008;7:64.
4. Duhagon MA, Hurt EM, Sotelo-Silveira JR, Zhang X, Farrar WL. Genomic profiling of tumor initiating prostatospheres. BMC Genomics 2010;11:324.
5. Gaviraghi M, Tunici P, Valensin S, Rossi M, Giordano C, Magnoni L, et al. Pancreatic cancer spheres are more than just aggregates of stem marker-positive cells. Biosci Rep 2011;31:45–55.
6. Hong SP, Wen J, Bang S, Park S, Song SY. CD44-positive cells are responsible for gemcitabine resistance in pancreatic cancer cells. Int J Cancer 2009;125:2323–31.
7. Ottinger S, Klöppel A, Rausch V, Liu L, Kallifatidis G, Gross W, et al. Targeting of pancreatic and prostate cancer stem cell characteristics by Crambe crambe marine sponge extract. Int J Cancer 2012; 130:1671–81.
8. Rajeshkumar NV, Rasheed ZA, García-García E, López-Ríos F, Fujiwara K, Matsui WH, et al. A combination of DR5 agonistic monoclonal antibody with gemcitabine targets pancreatic cancer stem cells and results in long-term disease control in human pancreatic cancer model. Mol Cancer Ther 2010;9:2582–92.
9. Chang CJ, Yang JY, Xia W, Chen CT, Xie X, Chao CH, et al. EZH2 promotes expansion of breast tumor initiating cells through activation of RAF1-β-catenin signaling. Cancer Cell 2011;19:86–100.
10. Cao R, Wang L, Wang H, Xia L, Erdjument-Bromage H, Tempst P, et al. Role of histone H3 lysine 27 methylation in Polycomb-group silencing. Science 2002;298:1039–43.
11. Viré E, Brenner C, Deplus R, Blanchon L, Fraga M, Didelot C, et al. The Polycomb group protein EZH2 directly controls DNA methylation. Nature 2006;16:871–74.
12. Santos-Rosa H, Caldas C. Chromatin modifier enzymes, the histone code and cancer. Eur J Cancer 2005;41:2381–402.
13. Toll AD, Dasgupta A, Potoczek M, Yeo CJ, Kleer CG, Brody JR , et al. Implications of enhancer of zeste homologue 2 expression in pancreatic ductal adenocarcinoma. Hum Pathol 2010;41:1205–9.
14. Ougolkov AV, Bilim VN, Billadeau DD. Regulation of pancreatic tumor cell proliferation and chemoresistance by the histone methyltransferase EZH2. Clin Cancer Res 2008;14:6790–6.
15. Xiong HQ, Carr K, Abbruzzese JL. Cytotoxic chemotherapy for pancreatic cancer: advances to date and future directions. Drugs 2006;66:1059–72.
16. Tan J, Yang X, Zhuang L, Jiang X, Chen W, Lee PL, et al. Pharmacologic disruption of polycomb-repressive complex 2-mediated gene repression selectively induces apoptosis in cancer cells. Genes Dev 2007;21:1050–63.
17. Hayden A, Johnson P, Packham G, Crabb SJ. S-adenosylhomocysteine hydrolase inhibition by 3-deazaneplanocin A analogues induces anti-cancer effects in breast cancer cell lines and synergy with both histone deacetylase and HER2 inhibition. Breast Cancer Res Treat 2011;127:109–19.
18. Giovannetti E, Funel N, Peters GJ, Del Chiaro M, Erozenci LA, Vasile E, et al. MicroRNA-21 in pancreatic cancer: correlation with clinical outcome and pharmacologic aspects underlying its role in the modulation of gemcitabine activity. Cancer Res 2010;70: 4528–38.
19. Miranda TB, Cortez CC, Yoo CB, Liang G, Abe M, Kelly TK, et al. DZNep is a global histone methylation inhibitor that reactivates developmental genes not silenced by DNA methylation. Mol Cancer Ther 2009;8:1579–88.
20. Giovannetti E, Del Tacca M, Mey V, Funel N, Nannizzi S, Ricci S, et al. Transcription analysis of human equilibrative nucleotide transporter-1 predicts survival in pancreas cancer patients treated with gemcitabine. Cancer Res 2006;66:3928–35.
21. Chou TC, Talalay P. Quantitative analysis of dose-effect relationships: the combined effects of multiple drugs or enzyme inhibitors. Adv Enzyme Regul 1984;22:27–55.
22. Giovannetti E, Mey V, Danesi R, Basolo F, Barachini S, Deri M, et al. Interaction between gemcitabine and topotecan in human non-small-cell lung cancer cells: effects on cell survival, cell cycle and pharmacogenetic profile. Br J Cancer 2005;92:681–9.
23. Mousavi SH, Moallem SA, Mehri S, Shahsavand S, Nassirli H, Malaekeh-Nikouei B. Improvement of cytotoxic and apoptogenic properties of crocin in cancer cell lines by its nanoliposomal form. Pharm Biol 2011;49:1039–45.
24. Mathews LA, Cabarcas SM, Hurt EM, Zhang X, Jaffee EM, Farrar WL. Increased expression of DNA repair genes in invasive human pancreatic cancer cells. Pancreas 2011;40:730–9.
25. Honeywell RJ, Giovannetti E, Peters GJ. Determination of the phosphorylated metabolites of gemcitabine and of difluorodeoxyuridine by LCMSMS. Nucleosides Nucleotides Nucleic Acids 2011;30:1203–13.
26. Yao J, Cai HH, Wei JS, An Y, Ji ZL, Lu ZP, et al. Side population in the pancreatic cancer cell lines SW1990 and CFPAC-1 is enriched with cancer stem-like cells. Oncol Rep 2010;23:1375–82.
27. Cao Q, Yu J, Dhanasekaran SM, Kim JH, Mani RS, Tomlins SA, et al. Repression of E-cadherin by the polycomb group protein EZH2 in cancer. Oncogene 2008;27:7274–84.
28. Padrón JM, van der Wilt CL, Smid K, Smitskamp-Wilms E, Backus HH, Pizao PE, et al. The multilayered postconfluent cell culture as a model for drug screening. Crit Rev Oncol Hematol 2000;36:141–57.
29. Xu CR, Cole PA, Meyers DJ, Kormish J, Dent S, Zaret KS. Chromatin "prepattern" and histone modifiers in a fate choice for liver and pancreas. Science 2011;332:963–6.
30. Chase A, Cross NC. Aberrations of EZH2 in cancer. Clin Cancer Res 2011;17:2613–8.
31. Varambally S, Dhanasekaran SM, Zhou M, Barrette TR, Kumar-Sinha C, Sanda MG, et al. The polycomb group protein EZH2 is involved in progression of prostate cancer. Nature 2002;419:624–9.
32. Kleer CG, Cao Q, Varambally S, Shen R, Ota I, Tomlins SA, et al. EZH2 is a marker of aggressive breast cancer and promotes neoplastic transformation of breast epithelial cells. Proc Natl Acad Sci U S A 2003;100:11606–11.
33. Chen Y, Xie D, Yin Li W, Man Cheung C, Yao H, Chan CY, et al. RNAi targeting EZH2 inhibits tumor growth and liver metastasis of pancreatic cancer *in vivo*. Cancer Lett 2010;297:109–16.
34. Zoabi M, Sadeh R, de Bie P, Marquez VE, Ciechanover A. PRAJA1 is a ubiquitin ligase for the polycomb repressive complex 2 proteins. Biochem Biophys Res Commun 2011;408:393–8.
35. Smits M, Nilsson J, Mir SE, van der Stoop PM, Hulleman E, Niers JM, et al. miR-101 is down-regulated in glioblastoma resulting in EZH2-induced proliferation, migration, and angiogenesis. Oncotarget 2010;1:710–20.
36. Conroy T, Desseigne F, Ychou M, Bouché O, Guimbaud R, Bécouarn Y, et al. FOLFIRINOX versus gemcitabine for metastatic pancreatic cancer. N Engl J Med 2011;364:1817–25.

Published OnlineFirst May 23, 2012; DOI: 10.1158/1535-7163.MCT-12-0037

37. Li D, Xie K, Wolff R, Abbruzzese JL. Pancreatic cancer. Lancet 2004;363:1049–57.
38. Gahr S, Ocker M, Ganslmayer M, Zopf S, Okamoto K, Hartl A, et al. The combination of the histone-deacetylase inhibitor trichostatin A and gemcitabine induces inhibition of proliferation and increased apoptosis in pancreatic carcinoma cells. Int J Oncol 2007;31:567–76.
39. Jones S, Zhang X, Parsons DW, Lin JC, Leary RJ, Angenendt P, et al. Core signaling pathways in human pancreatic cancers revealed by global genomic analyses. Science 2008;321:1801–6.
40. Kemp CD, Rao M, Xi S, Inchauste S, Mani H, Fetsch P, et al. Polycomb repressor complex-2 is a novel target for mesothelioma therapy. Clin Cancer Res 2012;18:77–90.
41. Aghdassi A, Sendler M, Guenther A, Mayerle J, Behn CO, Heidecke CD, et al. Recruitment of histone deacetylases HDAC1 and HDAC2 by the transcriptional repressor ZEB1 downregulates E-cadherin expression in pancreatic cancer. Gut 2012;61:439–48.
42. Simeone DM. Pancreatic cancer stem cells: implications for the treatment of pancreatic cancer. Clin Cancer Res 2008;14:5646–8.
43. Bao B, Ali S, Banerjee S, Wang Z, Logna F, Azmi AS, et al. Curcumin analog CDF inhibits pancreatic tumor growth by switching on suppressor microRNAs and attenuating EZH2 expression. Cancer Res 2012;72:335–45.
44. Crea F, Hurt EM, Mathews LA, Cabarcas SM, Sun L, Marquez VE, et al. Pharmacologic disruption of Polycomb Repressive Complex 2 inhibits tumorigenicity and tumor progression in prostate cancer. Mol Cancer 2011;10:40.
45. Rauchwerger DR, Firby PS, Hedley DW, Moore MJ. Equilibrative-sensitive nucleoside transporter and its role in gemcitabine sensitivity. Cancer Res 2000;60:6075–9.
46. Giovannetti E, Mey V, Nannizzi S, Pasqualetti G, Marini L, Del Tacca M, et al. Cellular and pharmacogenetics foundation of synergistic interaction of pemetrexed and gemcitabine in human non-small-cell lung cancer cells. Mol Pharmacol 2005;68:110–8.
47. Danesi R, Altavilla G, Giovannetti E, Rosell R. Pharmacogenomics of gemcitabine in non-small-cell lung cancer and other solid tumors. Pharmacogenomics 2009;10:69–80.
48. Van Moorsel CJ, Smid K, Voorn DA, Bergman AM, Pinedo HM, Peters GJ. Effect of gemcitabine and cis-platinum combinations on ribonucleotide and deoxyribonucleotide pools in ovarian cancer cell lines. Int J Oncol 2003;22:201–7.
49. Glazer RI, Knode MC, Tseng CK, Haines DR, Marquez VE. 3-Deazaneplanocin A: a new inhibitor of S-adenosylhomocysteine synthesis and its effects in human colon carcinoma cells. Biochem Pharmacol 1986;35:4523–7.

Published OnlineFirst May 23, 2012; DOI: 10.1158/1535-7163.MCT-12-0037

Molecular Cancer Therapeutics

Molecular Mechanisms Involved in the Synergistic Interaction of the EZH2 Inhibitor 3-Deazaneplanocin A with Gemcitabine in Pancreatic Cancer Cells

Amir Avan, Francesco Crea, Elisa Paolicchi, et al.

Mol Cancer Ther 2012;11:1735-1746. Published OnlineFirst May 23, 2012.